MNRAS 000, 1–20 (2015) Preprint 13 January 2016 Compiled using MNRAS LATEX style file v3.0

On the Formation of Galactic Black Hole Low-Mass X-ray Binaries

Chen Wang,[1,2] Kun Jia[1,2] and Xiang-Dong Li[1,2]⋆
[1] Department of Astronomy, Nanjing University, Nanjing 210046, China
[2] Key laboratory of Modern Astronomy and Astrophysics (Nanjing University), Ministry of Education, Nanjing 210046, China

arXiv:1601.02721v1 [astro-ph.HE] 12 Jan 2016

Accepted XXX. Received YYY; in original form ZZZ

ABSTRACT

Currently, there are 24 black hole (BH) X-ray binary systems that have been dynamically confirmed in the Galaxy. Most of them are low-mass X-ray binaries (LMXBs) comprised of a stellar-mass BH and a low-mass donor star. Although the formation of these systems has been extensively investigated, some crucial issues remain unresolved. The most noticeable one is that, the low-mass companion has difficulties in ejecting the tightly bound envelope of the massive primary during the spiral-in process. While initially intermediate-mass binaries are more likely to survive the common envelope (CE) evolution, the resultant BH LMXBs mismatch the observations. In this paper, we use both stellar evolution and binary population synthesis to study the evolutionary history of BH LMXBs. We test various assumptions and prescriptions for the supernova mechanisms that produce BHs, the binding energy parameter, the CE efficiency, and the initial mass distributions of the companion stars. We obtain the birthrate and the distributions of the donor mass, effective temperature and orbital period for the BH LMXBs in each case. By comparing the calculated results with the observations, we put useful constraints on the aforementioned parameters. In particular, we show that it is possible to form BH LMXBs with the standard CE scenario if most BHs are born through failed supernovae.

Key words: binaries: general − black hole physics − X-ray: binaries − stars: evolution

1 INTRODUCTION

There may be around 10^8-10^9 stellar-mass black holes (BHs) in the Galaxy (e.g., Brown & Bethe 1994; Timmes, Woosley & Weaver 1996), but only two dozen of them have been dynamically confirmed in X-ray binary (XRB) systems, in which a BH is accreting from its companion star (Remillard & McClintock 2006; Casares & Jonker 2014, for recent reviews). A large fraction of the BH XRBs are close binaries with orbital periods $P_{\rm orb} < 1$ day. The spectral types of the companion stars range from A2V to M1V, indicating that most of them are less massive than $2\,M_\odot$, so these XRBs are correspondingly classified as low-mass X-ray binaries (LMXBs). All known BH LMXBs are transient systems, spending most of their time in quiescence with X-ray luminosities below $\sim 10^{32}\,{\rm erg\,s^{-1}}$, and occasionally exhibiting outbursts when the X-ray luminosities can rise up to $\sim 10^{37}-10^{39}\,{\rm erg\,s^{-1}}$.

Galactic BH LMXBs are believed to evolve from primordial binaries consisting of a massive star and a low- or intermediate-mass companion (Li 2015, for a review). The standard formation scenario involves a common envelope (CE) phase, during which the binary's orbital separation reduces drastically due to the loss of the orbital kinetic energy (Paczynski 1976; van den Heuvel 1983), since the orbital separations of the present day binaries are orders-of-magnitude smaller than the radii that the massive primaries can reach during their evolution. When the primary star evolves and overflows its Roche lobe, mass transfer proceeds on a dynamical timescale because the primary is much more massive than the secondary. The secondary cannot accrete all the

⋆ E-mail: lixd@nju.edu.cn

© 2015 The Authors

mass transferred onto it, and an envelope forms enshrouding the two stars. Then the secondary star spirals into the envelope, and the orbital energy is used to expel the envelope (for reviews of CE evolution, see Taam & Sandquist 2000; Ivanova et al. 2013). If surviving the CE event, the binary can continue to evolve; otherwise the two stars would merge to be a single star. Though the CE stage is too short-lived to be detected, indirect observational evidence has emerged (e.g., Drake & Sarna 2003; Sion et al. 2012; Ivanova et al. 2013).

BHs are thought to be the evolutionary outcomes of sufficiently massive stars ($\gtrsim 20-25\,M_{\odot}$; e.g., Woosley & Weaver 1995; Fryer & Kalogera 2001). However, the envelope of such stars are generally too tightly bound for a low-mass secondary to expel (Podsiadlowski et al. 2003), thus a merger is more likely to take place, unless the primary has lost a significant fraction of its envelope before the CE phase through stellar winds (Wiktorowicz et al. 2013), or abnormally high values for the CE ejection efficiency are adopted (Kiel & Hurley 2006; Yungelson & Lasota 2008).

An alternative scenario is that the secondaries in BH LMXBs are initially intermediate-mass stars, which can eject the primary's envelope more easily. Observational evidence for this scenario comes from the CNO-processed material in XTE J1118+480 from its ultraviolet spectra (Haswell et al. 2002). It is, however, difficult for an intermediate-mass X-ray binary (IMXB) to evolve to short-period systems, unless some unusual angular momentum loss mechanisms are invoked (e.g., Justham et al. 2006; Chen & Li 2006). Meanwhile, these binaries reveal a discrepancy between the calculated effective temperatures and the observed spectral types of the donor stars. The reason lies in that nuclear burning in the center of an intermediate-mass star causes a higher effective temperature than an ordinary low-mass star, though it has lost a significant fraction of its mass during the evolution (Justham et al. 2006).

Clues to the initial mass range for the donors in BH LMXBs can be derived from the spin evolution of the BHs, since the BH spins increase with accretion (Thorne 1974). Two methods, i.e., X-ray continuum-fitting (Zhang, Cui, & Chen 1997; Davis et al. 2005) and modeling relativistic reflection (Fabian et al. 1989) have been employed to estimate the spins of about 20 BHs (McClintock et al. 2014; Fabian et al. 2014, and references therein). Assuming that BHs in LMXBs are born with negligible spins, Fragos & McClintock (2015) showed that the initial masses of the secondaries in short-period binaries are generally $\lesssim 1-2\,M_{\odot}$.

From another point of view, approaches have been taken in the study of CE evolution by refining the energy budget for the ejection as well as the core-envelope binding energy. For example, Ivanova (2002) argued that nuclear fusion should be added into the energy sources that may contribute to the envelope ejection. Podsiadlowski et al. (2010) proposed that a thermonuclear runaway which is caused by the mixing hydrogen from the secondary into the helium-burning shell of the primary would assist the ejection. When treating the binding energy of the envelope, Ivanova & Chaichenets (2011) pointed out that there might be mass outflows during the slow spiral-in stage, when the orbital energy is balanced with the enthalpy rather than merely the internal energy of the envelope. That treatment can lower the binding energy by a factor of $\sim 2-5$, and help allow for a low-mass companion to survive the CE phase. It is also noted that the value of the binding energy is sensitive to the definition of the boundary between the remnant core and the ejected envelope (e.g., Tauris & Dewi 2001). Ivanova (2011) advocated that, the He core of a giant would experience a thermal readjustment stage after the CE event. Thus the boundary between the remnant core and the ejected envelope can be determined as the place where the hydrogen burning shell had maximal compression prior to CE evolution.

Another issue in the formation of BH LMXBs is the mass range for the BH progenitors. Current supernova (SN) theories cannot reliably predict which stars form BHs instead of neutron stars (NSs), although they are generally thought to be more massive than $\sim 20-25\ M_{\odot}$. The BH masses in the 24 XRBs have been dynamically measured to be in the range of $\sim 2.7\,M_{\odot}$ to $\gtrsim 15\,M_{\odot}$ (Casares & Jonker 2014, and references therein). However, there is statistical evidence for the presence of a dearth of NSs or BHs with masses $\sim 2-5M_{\odot}$ (Bailyn et al. 1998; Özel et al. 2010, 2012; Farr et al. 2011; Kreidberg et al. 2012; Kiziltan et al. 2013). This is in contrast with the traditional thought that the distribution of BH masses should decay with mass (e.g., Fryer 1999; Fryer & Kalogera 2001), suggesting that the physics of SN explosions that lead to the formation of BHs is still unclear (Fryer et al. 2012; Belczynski et al. 2012). Recently, Kochanek (2014) argued that zero-age main sequence stars with mass $\gtrsim 17$ M$_{\odot}$ might experience an unsuccessful explosion and evolve to BHs, while stars with mass around $8-17\ M_{\odot}$ experience a successful SN explosion and become NSs. Though this bifurcation is not well understood and may be related to the compactness parameter that describes the density profile outside the iron core (O'Connor & Ott 2011; Clausen et al. 2015; Kochanek 2014), the failed SN mechanism can naturally account for the observed $\sim 2-5\,M_{\odot}$ gap between NSs and BHs. Horiuchi et al. (2014) proposed that this mechanism can interpret the red supergiant problem and the SN rate problem, which concerns the absence of red supergiants with masses $\sim 16-30\ M_{\odot}$ as the progenitors of Type IIP SNe, and the deficit of the observed cosmic SN rate compared to the observed cosmic star formation rate, respectively.

In this paper we investigate the formation of Galactic BH LMXBs incorporating the influence of the aforementioned factors with both stellar evolution and binary population synthesis (BPS) methods. In section 2, we calculate and compare the binding energy parameters in various models, which are then used in our BPS study. In section 3, we introduce the assumptions and prescriptions adopted in our BPS calculations. The results in various kinds of models are presented and compared with observations in section 4. We summarize the results and discuss their implications in section 5.

2 THE BINDING ENERGY PARAMETER

In the standard CE model the change in the binary's orbital energy $\Delta E_{\rm orb}$ is responsible for the ejection of the CE, which is described by the following equations (Webbink 1984),

$$E_{\rm bind} = \alpha_{\rm CE}\Delta E_{\rm orb}, \tag{1}$$

and

$$\Delta E_{\rm orb} = \frac{GM_{\rm core}M_2}{2a_{\rm f}} - \frac{GM_1M_2}{2a_{\rm i}}, \tag{2}$$

where $E_{\rm bind}$ is the binding energy of the envelope, $\alpha_{\rm CE}$ the efficiency of converting the orbital energy to kinetic energy to eject the CE, G the gravitational constant, M_1 the primary's mass and $M_{\rm core}$ its core mass, M_2 the mass of the secondary, and $a_{\rm i}$ and $a_{\rm f}$ the orbital separations just before and after the CE phase, respectively.

When only gravitational binding energy is considered, $E_{\rm bind}$ is given by

$$E_{\rm bind} = \int_{M_{\rm core}}^{M_1} -\frac{GM(r)}{r}dm. \tag{3}$$

If the internal energy of the stellar matter (including both thermal energy and recombination energy) also contributes to the binding energy, then we have

$$E_{\rm bind} = \int_{M_{\rm core}}^{M_1} \left[-\frac{GM(r)}{r} + U\right] dm, \tag{4}$$

where U is internal energy (Han et al. 1994). Recently, Ivanova & Chaichenets (2011) proposed a modified energy criterion taking into account the mass outflows during the spiral-in stage. In this so-called enthalpy model, the binding energy is expressed as

$$E_{\rm bind} = \int_{M_{\rm core}}^{M_1} \left[-\frac{GM(r)}{r} + U + \frac{P}{\rho}\right] dm, \tag{5}$$

where P and ρ are the pressure and the density of the gas, respectively. Since the P/ρ term is non-negative, the absolute value of $E_{\rm bind}$ becomes smaller in this case.

For convenience, de Kool (1990) introduced a parameter λ characterizing the central concentration of the donor's envelope to describe the binding energy:

$$E_{\rm bind} = -\frac{GM_1M_{\rm env}}{\lambda a_{\rm i} r_{\rm L}}, \tag{6}$$

where $M_{\rm env}$ is the mass of the donor star's envelope, and $r_{\rm L} = R_{\rm L}/a_{\rm i}$ is the ratio of the Roche lobe radius and the orbital separation at the onset of CE. Generally, once a star fills its Roche lobe, $a_{\rm i}r_{\rm L}$ is taken to be the stellar radius.

Combining Eqs. (3)–(6), one can obtain different λs from the gravitational binding energy, the total energy and the enthalpy prescriptions, namely $\lambda_{\rm g}$, $\lambda_{\rm b}$ and $\lambda_{\rm h}$, respectively. We calculate their values using an updated version (7624) of the Modules for Experiments in Stellar Astrophysics (MESA) (Paxton et al. 2011, 2013, 2015) evolution code. We consider stars with initial masses in the range of $19-60\,M_\odot$, which securely covers the range of the stellar-mass BH progenitors (more massive stars produce negligible BHs according to the initial mass function and will evolve to Wolf-Rayet (WR) stars with almost all the hydrogen envelopes lost due to strong stellar winds). The chemical composition of the stars is taken to be $X = 0.7$ and $Z = 0.02$. The mixing length parameter $\alpha = l/H_{\rm p}$ is set to be 2.0. For massive stars, stellar winds may have non-ignorable influence on the λ parameter (Podsiadlowski et al. 2003), but their loss rates have not been accurately determined. Here, we adopt two prescriptions for the wind loss rate. The first one is taken from Hurley et al. (2000) and Vink (2001) for O and B stars in different stages, denoted as Wind1 hereafter, while the other one, denoted as Wind2, adopts the maximum value of the prescriptions above in all the evolutionary stages, to be consistent with Xu & Li (2010a,b), and to set an upper limit for the influence of the stellar wind. The effect of stellar rotation is ignored, because in our calculation for LMXB formation, CE evolution usually occurs during Case C mass transfer when the primary star has evolved to be a supergiant star with very slow rotation due to stellar evolution and/or tidal synchronization.

Our calculations show that the evolution of $\lambda_{\rm h}$, $\lambda_{\rm b}$, and $\lambda_{\rm g}$ generally have the similar trend in most of the evolutionary stages, i.e., decreasing with increasing stellar radius. However, for stars less massive than $30\,M_\odot$, λs increase again when they have ascended the asymptotic giant branch and developed a deep envelope (see also Podsiadlowski et al. 2003). As an illustration, Fig. 1 shows different λ values as a function of the stellar radius R for a $20\,M_\odot$ star, and Fig. 2 shows the $\lambda_{\rm h}$ values as a function of the stellar radius for stars with different masses. The solid and dashed lines correspond to the Wind1 and Wind2 prescriptions, respectively. In Fig. 1 the red, blue, and green lines describe the evolution of $\lambda_{\rm h}$, $\lambda_{\rm b}$, and $\lambda_{\rm g}$ respectively in each case. It is seen that the values of λ with the Wind1 prescription are about three times as large as those with the Wind2 prescription (the binding energy with the Wind1 prescription is half of the value with the Wind2 prescription considering different envelope masses), indicating that the binding energy parameter for massive stars is sensitive to wind loss (Podsiadlowski et al. 2003). We plot the core mass against the stellar radius in Fig. 3, and list the stellar parameters along the evolutionary tracks in Table 1 in the two cases.

We also use an updated stellar evolution code called EV originally developed by Eggleton (1971, 1972) to calculate the values of λs, and find that they are several times smaller than those with the MESA code in the Wind2 case (see also Xu & Li 2010a,b). The reason for this difference is that stars are generally more compact (especially for stellar structure within the hydrogen burning shell) during late evolution when modeled with the EV code. We choose to use the results with the MESA code in the following because it adopts much denser grids for stellar structure than the EV code.

Justham et al. (2006) pointed out that a low-mass ($< 1\,M_\odot$) star is unable to eject the BH progenitor's envelope unless $\lambda \gtrsim 0.15$. In our calculation, this condition could be achieved for both $\lambda_{\rm h}$ and $\lambda_{\rm b}$ if the masses of the BH progenitors are $< 25\ M_\odot$. Binaries with more massive progenitor stars are unable to survive CE evolution even if $\lambda_{\rm h}$ is adopted (see also Fig. 2).

3 BINARY POPULATION SYNTHESIS

We use an updated version of the BPS code developed by Hurley et al. (2002) to study the formation of BH LMXBs. The code originates from the rapid single-star evolution code written by Hurley et al. (2000). It involves various kinds of processes such as mass transfer, accretion, CE evolution, SN kicks, tidal interactions, and angular momentum loss. We have made quite a few modifications of the BPS code to follow the formation and evolution of XRBs (Shao & Li 2014). We briefly describe some considerations adopted in this work.

3.1 CE evolution

Given the binding energy parameter λ, we can estimate the post-CE separation with the following equation:

$$\frac{a_{\rm f}}{a_{\rm i}} = \frac{M_{\rm core} M_2}{M_1} \frac{1}{M_2 + 2M_{\rm env}/\alpha_{\rm CE}\lambda r_{\rm L}}. \tag{7}$$

If neither the He core nor the secondary star fills its Roche lobe, the binary is regarded to survive the CE phase and can continue to evolve.

Generally the value of $\alpha_{\rm CE}$ is less than unity, and there is indication that the CE efficiency could be low (Ohlmann et al. 2016). Moreover, it may vary with stellar structure and the binary parameters. Indeed, it has been suggested that $\alpha_{\rm CE}$ may depend on the component mass and the orbital period in the studies of the formation of post-CE white dwarf binaries (e.g., De Marco et al. 2011; Davis et al. 2012). However, it is not known whether this can be applied to more massive binaries, so we still adopt constant values (1 and 0.2) for $\alpha_{\rm CE}$. It is noted that $\alpha_{\rm CE}$ and λ are usually combined to affect CE evolution.

3.2 Remnant mass

Besides CE evolution, the SN explosions play an important role in the formation of BH LMXBs. The SN mechanisms are relevant to both the formation rate of XRBs and the mass distribution of the remnant BHs.

When determining the BH masses $M_{\rm BH}$, one needs to account for the measured masses of known BHs and the $\sim 2-5\,M_\odot$ gap between the NS and BH masses without any fine-tuning of stellar mass loss. We consider both the prescriptions based on the neutrino-driven convection-enhanced SN mechanism, which is called the rapid SN mechanism, and the failed SN mechanism. In the former case the gravitational remnant mass is described by (Fryer et al. 2012),

$$M_{\rm rem} = 0.9 M_{\rm rem,bar} = 0.9(M_{\rm proto} + M_{\rm fb}). \tag{8}$$

Here $M_{\rm proto} = 1.0\,M_\odot$ is the mass of the proto-compact object and

$$\begin{cases} M_{\rm fb} = 0.2\ M_\odot & M_{\rm CO} < 2.5\,M_\odot \\ M_{\rm fb} = 0.286 M_{\rm CO} - 0.514\ M_\odot & 2.5\,M_\odot \le M_{\rm CO} < 6.0\,M_\odot \\ M_{\rm fb} = f_{\rm fb}(M_1 - M_{\rm proto}) & M_{\rm CO} \ge 6\,M_\odot, \end{cases} \tag{9}$$

with

$$\begin{cases} f_{\rm fb} = 1.0 & 6.0\ M_\odot \le M_{\rm CO} < 7.0\ M_\odot \\ f_{\rm fb} = a_1 M_{\rm CO} + b_1 & 7.0\ M_\odot \le M_{\rm CO} < 11.0\ M_\odot \\ f_{\rm fb} = 1.0 & M_{\rm CO} \ge 11.0\ M_\odot, \end{cases} \tag{10}$$

where $M_{\rm CO}$ is the CO core mass, $a_1 = 0.25 - 1.275/(M_1 - M_{\rm proto})$, and $b_1 = -11a_1 + 1$.

The latter prescription is under the assumption that the BH formation is controlled by the compactness of the stellar core at the time of collapse: low compactness stars are more likely to explode as SNe and produce NSs, while high-compactness stars are more likely to evolve to failed SNe that produce BHs (O'Connor & Ott 2011). In this case we assume $M_{\rm BH} = M_{\rm He}$ or $M_{\rm CO}$, where $M_{\rm He}$ is the He core masses prior to core collapse (e.g., Smith et al. 2011; Smith & Arnett 2014; Shiode & Quataert 2014; Sukhbold & Woosley 2014; Clausen et al. 2015; Kochanek 2014, 2015). The value of $M_{\rm He}$ is determined as follows (Hurley et al.

2000, for a detailed description). First, the core mass $M_{\rm c}$ at the end of the Hertzsprung-gap is set according to the initial mass of the star (see Eq. 28 of Hurley et al. 2000). Then the evolution of the core mass during the giant branch is determined by combining the power-law core mass-luminosity relation

$$L = \min(BM_{\rm c}^{q}, DM_{\rm c}^{p}), \tag{11}$$

where $p = 5$, $q = 2$, and B and D depend on the stellar mass, and the energy conservation equation for hydrogen burning

$$L = EX_{\rm e}\dot{M}_{\rm c}, \tag{12}$$

where $X_{\rm e}$ is the envelope mass fraction of hydrogen and E is the specific energy release. Thus

$$\dot{M}_{\rm c} = \min(A_{\rm H}BM_{\rm c}^{q}, A_{\rm H}DM_{\rm c}^{p}), \tag{13}$$

where $A_{\rm H} = 1/EX_{\rm e}$ represents hydrogen rate constant. A similar procedure is adopted to calculate the CO core mass, with $A_{\rm H}$ replaced by $A_{\rm He} = 7.66 \times 10^{-5} M_{\odot} L_{\odot}^{-1}$ Myr^{-1}.

In all of the cases we require that $M_{\rm BH} \geq 3M_{\odot}$. We do not consider the formation of BHs by accretion-induced collapse of NSs in XRBs. We also assume that a natal "kick" is imparted on the newborn BHs, similar as NSs. The kick velocity is set to be inversely proportional to the remnant mass, i.e., $V_{\rm kick}({\rm BH}) = (3M_{\odot}/M_{\rm BH})V_{\rm kick}({\rm NS})$, where $V_{\rm kick}({\rm NS})$ is the kick velocity for NSs, which follows a Maxwellian distribution with $\sigma = 265$ km s^{-1} (Hobbs et al. 2005).

3.3 Initial parameters

We consider the BH LMXBs evolved from primordial binaries with both incipient low-mass and intermediate-mass secondaries. We assume a constant star formation rate of $5\,M_{\odot}{\rm yr}^{-1}$ (Smith et al. 1978), and evolve 10^7 primordial binaries with the primary mass (M_1) ranging from $19\,M_{\odot}$ to $60\,M_{\odot}$ following the Kroupa et al. (1993) initial mass function, and the secondary mass (M_2) from $0.1\,M_{\odot}$ to $6\,M_{\odot}$. For the initial mass ratio $q = M_2/M_1$, we consider both flat distribution $n(q) = 1$ with q randomly distributed between 0 and 1, and a "twin"-like distribution with $n(q) \propto q$. The initial separation a of the binary components varies between $3\,R_{\odot}$ and $10^4\,R_{\odot}$, with a flat distribution for $\ln a$. All binaries are assumed to be initially in circular orbits. We stop the calculation when the donor mass in LMXBs drops down to $0.1\,M_{\odot}$, or the evolution time exceeds 15 Gyr. We summarize the models and the prescriptions employed in Table. 2.

4 RESULTS

4.1 The donor mass distribution

We first consider the formation of BHs via the rapid SN mechanism. In this case the progenitor stars are usually more massive than $28\,M_{\odot}$ in binaries. For such massive stars the binding energy of the envelope is so large that with $\lambda = \lambda_{\rm g}$ a low-mass secondary inevitably merges with the He core of the primary, and no successful BH LMXBs can form (see also Podsiadlowski et al. 2003). So in models A1 and A2 we set $\alpha_{\rm CE} = 1$ with $\lambda = \lambda_{\rm b}$ and $\lambda_{\rm h}$, respectively. The distributions of the donor mass of the resultant BH XRBs at current epoch are plotted in the left and right panels of Fig. 4, respectively. To reveal the donor mass distribution in different scale, the donor masses are confined within $0-6\,M_{\odot}$ and $0-2\,M_{\odot}$ in the upper and lower panels of the figure, respectively. The solid and dashed red lines represent the results with the λs obtained with the Wind1 and Wind2 prescriptions, respectively. Also displayed is the distribution of the observed BH LMXBs with the black line (data taken from Wiktorowicz et al. 2013; Fragos & McClintock 2015). The number of the BH XRBs is calculated by multiplying the formation rate with the duration in a specific stage. We only display the sources which are subject to the thermal-viscous instability in an X-ray irradiated accretion disk and "assumed" to be transient (Lasota 2001; Lasota et al. 2008)[1]. They include almost all BH LMXBs produced. The exceptions are the systems comprised of intermediate-mass donors or with extremely short periods, which are not relevant here. In model A1 and A2, the donors of persistent sources locate in the mass range of $4-6\,M_{\odot}$, and their total number is comparable with that of transient sources. When $\lambda = \lambda_{\rm b}$, most BH XRBs harbor an intermediate-mass donor star (with mass $M > 3M_{\odot}$), implying that lower-mass secondaries are unlikely to survive CE evolution. The corresponding formation rate of the BH XRBs is too low ($\sim 2.80 \times 10^{-8}$ yr^{-1}) to account for the observed systems in the Galaxy. When $\lambda = \lambda_{\rm h}$, the formation rate enhances a bit ($\sim 3.57 \times 10^{-8}$ yr^{-1}), and the donor mass distribution peaks at around $4\,M_{\odot}$. It is seen that in both cases the distributions significantly deviate from the observed one. The calculated orbital period distributions are too long (> 1 day) to be consistent with observations (see Fig. 12 below). These results clearly disfavors the rapid SN mechanism, so in the following we only consider the failed SN mechanism.

In models B1 and B2, we assume $M_{\rm BH} = M_{\rm He}$ and a flat mass ratio distribution with $\lambda = \lambda_{\rm b}$ and $\lambda = \lambda_{\rm g}$, respectively.

[1] We caution that, despite the thermal-viscous instability seem to succeed in explaining the dichotomy between the transient and the persistent LMXBs averaged over a long enough period of time (Coriat et al. 2012), it may not be the only mechanism, other mechanisms (e.g., irregular mass injection from the low-mass, fully convective donor stars) can also be at work.

We present the calculated distributions of the donor mass for the two models and compare them with observations in Fig. 5 (left: B1; right: B2). Here the red and blue lines correspond to $\alpha_{\rm CE} = 1$ and 0.2, respectively, and the line styles are same as in Fig. 4. With the failed SN mechanism the masses of the BH progenitors can be lower than $20\,M_\odot$, so it is easier for low-mass secondaries to survive the CE phase. From the left panel of Fig. 5 we see that in the cases of Wind1/$\alpha_{\rm CE} = 1$, Wind2/$\alpha_{\rm CE} = 1$, and Wind1/$\alpha_{\rm CE} = 0.2$ the donor mass peaks at $\sim 0.6\ M_\odot$, matching the observational data, while in the case of Wind2/$\alpha_{\rm CE} = 0.2$, the donor masses cluster around $1.2 - 1.4\ M_\odot$, larger than the observed peak. This is simply because more massive donor stars are required to survive the CE evolution when the product $\alpha_{\rm CE}\lambda$ is lower. However, larger $\alpha_{\rm CE}\lambda$ does not always necessarily lead to larger number of BH LMXBs, since the formation of a BH XRB strongly depends on the orbital separation just before and after the CE phase. With the same initial orbital periods, larger $\alpha_{\rm CE}\lambda$ results in wider post-CE orbits, which may cause the subsequent Roche lobe overflow to be postponed, reducing the X-ray lifetime and thus the number of XRBs.

Figure 6 shows the birthrates of the BH XRBs as a function of the initial donor mass in each case. We mention that, although the BH XRB birthrates can be as high as $\sim 6 \times 10^{-6}$ yr^{-1}, the birthrates of those with incipient low-mass donors are several times lower.

We use the Kolmogorov-Smirnov (KS) test to quantitatively compare the the univariate distributions of the calculated and measured donor mass. The KS statistic D quantifies a distance between the empirical distribution functions of the two samples. The null hypothesis that the two distributions are drawn from the same one is rejected at a significance level α if $D > D_{\rm cr}(\alpha)$ (Feigelson & Jogesh 2012). In Table 2 we list the calculated values of D and $D_{\rm cr}(\alpha)$ for all models (except models A1 and A2 because of too few data points) in the case of Wind2/$\alpha_{\rm CE} = 1$ at $\alpha = 0.001$ and 0.05.

Figure 7 shows the donor mass distributions for models C1 (left panel) and C2 (right panel) under the assumptions that $M_{\rm BH} = M_{\rm He}$ and $\lambda = \lambda_{\rm h}$. In models C1 and C2 we adopt a flat distribution of the initial mass ratio and a "twin" distribution (Pinsonneault & Stanek 2006; Kobulnicky & Fryer 2007, see however, Cantrell & Dougan 2014), respectively. Here we confine the donor masses within the range of $0 - 2\,M_\odot$ because of the small number of XRBs with more massive donor stars. Figure 7 shows that the peak of the donor mass distribution in the cases of Wind1/$\alpha_{\rm CE} = 1$, Wind2/$\alpha_{\rm CE} = 1$, and Wind1/$\alpha_{\rm CE} = 0.2$ is $\sim 0.6\,M_\odot$, but shifts towards $\sim 1.0\,M_\odot$ in the case of Wind2/$\alpha_{\rm CE} = 0.2$, roughly in accordance with Fig. 5. This is also reflected by their similar D values. To see whether the resultant BH LMXBs evolve from incipient low- or intermediate-mass binaries, we repeat the calculation with the initial donor mass confined to be $< 2\ M_\odot$ and $< 1\ M_\odot$ respectively. The results in model C1 (with the Wind2 prescription) are plotted in Fig. 8. It is clearly seen that the total number of the BH LMXBs evolved from the primordial binaries with the initial donor mass $M_{2initial} < 2\,M_\odot$ is almost the same as in the left panel of Fig. 7, so we can safely conclude that almost all the BH LMXBs in our calculation have incipient low-mass secondaries. Although the BH XRBs with low-mass donors have a lower birthrate than those with intermediate-mass donors, it is compensated by their long X-ray lifetimes. Figure 7 also indicates that assuming a $n(q) \propto q$ distribution (model C2) leads to less efficient formation of BH LMXBs than with a flat q distribution because of less progenitor binaries with low-mass secondary stars. Figure 9 shows the distribution of the orbital period vs. the donor mass (left panel), and the distribution of the mass transfer rate vs. the donor mass (right panel) in model C1. The color scale represents the relative number of the XRBs in a parameter space. It can be seen that the majority of BH XRBs are short-period (< 1 day) systems with mass transfer rates below $10^{-9} M_\odot {\rm yr}^{-1}$.

The above results are based on the hypothesis that the BH mass is equal to its progenitor's He core mass at the time of core bounce. To check the effect of another choice of the remnant mass, we construct models D1 and D2, which are same as models C1 and C2 except with $M_{\rm rem} = M_{\rm CO}$, respectively. The donor mass distributions are shown in Fig. 10. We find that the formation rate in mode D1 decreases to about half that in model C1, and the peak of the donor mass distribution extends to a broader range compared with Fig. 6. The remnant mass influences the formation of the BH LMXBs by determining the Roche lobe size after the SN explosion. Figure 11 shows the distributions of the BH masses under the two choices. The red and blue lines represent the results in models C1 and D1, which peak at $\sim 6.6 - 7\,M_\odot$ and $\sim 5.0 - 5.4\,M_\odot$, respectively. Özel et al. (2010) have analyzed the data of 16 BH X-ray transients, and found that the observed BH masses can be best described by a narrow distribution at $7.8 \pm 1.2\,M_\odot$, which is obviously more compatible with the result in model C1.

4.2 Distribution of the orbital period and the effective temperature of the donor stars

In Figs. 12 we show the calculated distributions of the orbital period and the effective temperature of the donor stars in model A. The color scale represents the relative number of the XRBs. We also plot the measured orbital periods and effective temperatures of the donors for Galactic BH LMXBs. In Fig. 12 for models A1 (left panel) and A2 (right panel), the observed distribution obviously deviates from the calculation, showing a tendency towards lower temperature. The reason is that, as stated before, most of the BH LMXBs in models A1 and A2 descended from IMXBs, so the donor star is likely to have a higher temperature than an originally low-mass star. We get similar results for model B2 with $\alpha = 0.2$. In other models the calculated orbital periods are more compatible with observations. We also use the KS test to quantitatively compare the calculated and observed distributions, and the results for models B1, B2, C1, and D1 are shown in Table 3. We can see that, except model B2 with $\alpha_{\rm CE} = 0.2$, other models are all acceptable. We show the distributions in the best-fit model C1 in Fig. 13.

5 DISCUSSION AND CONCLUSIONS

Previous studies have already demonstrated that it is hard to produce compact BHXRBs consisting of an initially low-mass companion with the standard formation scenario, since the companion star is unable to expel the CE (e.g., Portegies Zwart et al. 1997; Kalogera 1999; Podsiadlowski et al. 2003; Kiel & Hurley 2006, see however, Yungelson & Lasota 2008; Wiktorowicz et al. 2013). However, the orbital periods, the donors' spectral types, and the measured spins of quite a few BHs strongly suggest that in the incipient binaries the donor stars are likely to be of low-mass.

We construct a series of models to explore the plausible solutions to the above-mentioned puzzle. The factors we have taken into account include the binding energy parameter λ, the CE efficiency $\alpha_{\rm CE}$, the SN mechanisms for BH formation, and the distribution of the mass ratio. By adopting different choices of these prescriptions, we examine their roles in the formation of BH LMXBs by comparing the calculated parameter distributions with observations. Our calculations show that the λ-values strongly depend on the stellar mass and the evolutionary stage. Generally $\lambda_{\rm h}$ is several times larger than $\lambda_{\rm g}$ and $\lambda_{\rm b}$, and this can help the binary to avoid merging during the CE evolution without invoking unphysically high values of $\alpha_{\rm CE}$. However, we fail to reproduce the observational characteristics of Galactic BH LMXBs based on the rapid SN mechanism even with $\lambda_{\rm h}$ adopted, since the BH progenitors are still too massive ($\gtrsim 28\,M_{\odot}$) in this scenario. We then consider the alternative failed SN mechanism, and assume that the remnant BH mass equals the He or CO core mass of the primary. This time we obtain more satisfactory results, with the distributions of the donor mass, temperature and orbital period for the current binaries largely consistent with observations. In particular, most BH LMXBs in this case originate from primordial binaries with incipient low-mass ($< 2\ M_{\odot}$) secondary stars, compatible with the requirement derived from the spin estimates of several BHs in LMXBs. Finally, all models predict that most BH LMXBs are transient sources due to thermal instability in the accretion disks. Thus, in the framework of the failed SN mechanism, it is possible to reproduce the Galactic BH LMXBs with normal value of $\alpha_{\rm CE} = 1$.

Realizing the uncertainties in the treatment of CE evolution, we also check the results by adopting a small $\alpha_{\rm CE} = 0.2$ in each case. Our results demonstrate that, when $\alpha_{\rm CE}\lambda$ is large enough for a low-mass star to survive the CE phase, the donor mass distribution is not sensitive to the choice of λ or $\alpha_{\rm CE}$, which affects the number and birthrate of the produced BH LMXBs. However, for very small $\alpha_{\rm CE}\lambda$, the donor mass distribution strongly depends on the value of λ or $\alpha_{\rm CE}$, because surviving the CE phase becomes paramount and difficult. In addition, the prescription of the BH mass with the He core mass leads to better match of the observations than with the CO core mass.

Our results provide useful constraints on the formation process of BH LMXBs, but are subject to many uncertainties in both observational and theoretical aspects. When comparing the calculated results with observations, one needs to be cautious that this comparison is influenced by small number statistics as well as selection effects. Currently there are around 20 dynamically confirmed stellar-mass BHs. It is not known whether they are correctly representative of the overall population in the Galaxy. Most BH LMXBs are transient sources, and we are lack of thorough understanding of their outburst characteristics (including the peak luminosity and its relation with other parameters, and the duty cycles) and the physical mechanisms (Remillard & McClintock 2006). To make things more complicated, a new class of very faint X-ray transients were recently discovered with peak luminosities of only $\sim 10^{34} - 10^{36}$ ergs^{-1} (Wijnands et al. 2006). Further more, considering the selection effect that luminous sources are more likely to be observed, we may expect that a large fraction of the LMXBs possess even lower-mass donor stars than the current sample, because they are relatively dim in X-rays even during outbursts.

There are also big uncertainties in modeling the evolutionary sequences of compact star binaries. We take into account $\lambda_{\rm h}$ in calculating the binding energy of the envelope (see also Wong et al. 2014), but its credibility is controversial and there are arguments both for and against it in the literature, let alone the definition of the core-envelope boundary from which the binding energy is integrated (see Ivanova et al. 2013, for a discussion). It is also highly uncertain whether the CE efficiency $\alpha_{\rm CE}$ is constant or depends on other physical parameters. De Marco et al. (2011) and Davis et al. (2012) suggested that it may decrease with increasing mass ratio, but this effect has not been confirmed in modeling the SDSS post-CE binary population (e.g., Zorotovic et al. 2011) and needs further verification. Even if true, the physics behind it is not clear, and numerical simulations in 3D of CE evolution are eagerly required to resolve this issue. As to the SN and the BH formation mechanisms, our results base on the suggestion that stars of mass $\sim 17 - 25 M_{\odot}$ die in failed SNe leaving a BH (Kochanek 2014; Horiuchi et al. 2014). The model still needs to be tested by both 3D numerical simulations of the collapse of massive stars and targeted field surveys for SNe in nearby galaxies.

Obviously a thorough investigation on the evolutionary history of BH LMXBs needs to incorporate BPS with the aforementioned input physics in a self-consistent way.

ACKNOWLEDGEMENTS

We are grateful to an anonymous referee for helpful comments. This work was supported by the Natural Science Foundation of China under grant numbers 11133001 and 11333004, and the Strategic Priority Research Program of CAS (under grant number XDB09000000).

REFERENCES

Bailyn, C. D., Jain, R. J., Coppi, P., & Orosz, J. A. 1998, ApJ, 499, 367
Belczynski, K., Wiktorowicz, G., Fryer, C. L., Holz, D. E., & Kalogera, V. 2012, ApJ, 757, 91
Brown, G. E., & Bethe, H. A. 1994, ApJ, 423, 659
Cantrell, A. G., & Dougan, T. J. 2014, MNRAS, 445, 2028
Casares, J. & Jonker, P. G. 2014, Spa. Sci. Rev., 183, 223
Chen, W.-C., & Li, X.-D. 2006, MNRAS, 373, 305
Clausen, D., Piro, A. L., & Ott, C. D. 2015, ApJ, 799, 190
Coriat, M., Fender, R. P., & Dubus, G. 2012, MNRAS, 424, 1991
Davis, S. W., Blaes, O. M., Hubeny, I., & Turner, N. J. 2005, ApJ, 621, 372
Davis, P. J., Kolb, U., & Knigge, C. 2012, MNRAS, 419, 287
de Kool, M. 1990, ApJ, 358, 189
De Marco, O., Passy, J.-C., Moe, M., Herwig, F., Mac Low M.-M., Paxton, B. 2011, MNRAS, 411, 2277
Drake, J. J., & Sarna, M. J. 2003, ApJ, 594, 55
Eggleton, P. P. 1971, MNRAS, 151, 351
Eggleton, P. P. 1972, MNRAS, 156, 361
Fabian, A. C., Parker, M. L., Wilkins, D. R., et al. 2014, MNRAS, 439, 2307
Fabian, A. C., Rees, M. J., Stella, L., & White, N. E. 1989, MNRAS, 238, 729
Farr, W. M., Sravan, N., Cantrell, A. et al. 2011, ApJ, 741, 103
Feigelson, E. D., & Jogesh, B. G. 2012, Modern Statistical Methods for Astronomy, Cambridge University Press (Cambridge, UK)
Fragos, T., & McClintock, J. E. 2015, ApJ, 800, 17
Fryer, C. L. 1999, ApJ, 522, 413
Fryer, C. L., Belczynski, K., Wiktorowicz, G. et al. 2012, ApJ, 749, 91
Fryer, C. L., & Kalogera, V. 2001, ApJ, 554, 548
Han, Z., Podsiadlowski, P., & Eggleton, P. P. 1994, MNRAS, 270, 121
Han, Z., Podsiadlowski, P., Maxted, P. F. L., Marsh, T. R., & Ivanova, N. 2002, MNRAS, 336, 449
Han, Z., Podsiadlowski, P., Maxted, P. F. L., & Marsh, T. R. 2003, MNRAS, 341, 669
Haswell, C. A., Hynes, R. I., King, A. R., & Schenker, K. 2002, MNRAS, 332, 928
Hobbs, G., Lorimer, D. R., Lyne, A. G., & Kramer, M. 2005, MNRAS, 360, 974
Horiuchi, S., Nakamura, K., Takiwaki, T., Kotake, K., Tanaka, M. 2014, MNRAS, 445, L99
Hurley, J. R., Pols, O. R., & Tout, C. A. 2000, MNRAS, 315, 543
Hurley, J. R., Tout, C. A., & Pols, O. R. 2002, MNRAS, 329, 897
Ivanova, N. 2002, PhD thesis, Oxford University
Ivanova, N. 2006, ApJ, 653, L37
Ivanova, N. 2011, ApJ, 730,76
Ivanova, N., & Chaichenets, S. 2011, ApJ, 731, L36
Ivanova, N., Justham, S., Chen, X., et al. 2013, A&AR, 21, 59
Justham, S., Rappaport, S., & Podsiadlowski, P. 2006, MNRAS, 366, 1415
Kalogera, V. 1999, ApJ, 521, 723
Kiel, P. D., & Hurley, J. R. 2006, MNRAS, 369, 1152
Kiziltan, B., Kottas, A., De Yoreo, M., & Thorsett, S. E. 2013, ApJ, 778, 66
Kobulnicky, H. A., & Fryer, C. L. 2006, ApJ, 670, 747
Kochanek, C. S. 2014, ApJ, 785, 28
Kochanek, C. S. 2015, MNRAS, 446, 1213
Kreidberg, L., Bailyn, C. D., Farr, W. M., & Kalogera, V. 2012, ApJ, 757, 36
Kroupa, P., Tout, C. A., & Gilmore, G. 1993, MNRAS, 262, 545
Lasota, J.-P. 2001, New Astron. Rev., 45, 449
Lasota, J.-P., Dubus, G., & Kruk, K. 2008, A&A, 486, 523
Li, X.-D. 2015, New Astron. Rev., 64-66, 1
McClintock, J. E., Narayan, R., & Steiner, J. F. 2014, Space Sci. Rev., 183, 295
O'Connor, E., & Ott, C. D. 2011, ApJ, 730, 70
Ohlmann, S. T., Röpke, F. K., Pakmor, R., & Springel, V. 2016, ApJ, 816, L9
Özel, F., Psaltis, D., Narayan, R., & McClintock, J. E. 2010, ApJ, 725, 1918
Özel, F., Psaltis, D., Narayan, R., & Santos Villarreal, A. 2012, ApJ, 757, 55
Paczynski, B. 1976, in IAU Symposium, Vol. 73, Structure and Evolution of Close Binary Systems, ed. P. Eggleton, S. Mitton, & J. Whelan (Dordrecht, D. Reidel Publishing Co.), p. 75
Paxton, B., Bildsten, L., Dotter, A., et al. 2011, ApJS, 192, 3
Paxton, B., Cantiello, M., Arras, P., et al. 2013, ApJS, 208, 4
Paxton, B., Marchant, P., Schwab, J., et al. 2015, ApJS, 220, 15
Pinsonneault, M. H., & Stanek, K. Z. 2006, ApJ, 639, L67
Podsiadlowski, P., Rappaport, S., & Pfahl, E.D. 2002, ApJ, 565, 1107
Podsiadlowski, P., Rappaport, S., & Han, Z. 2003, MNRAS, 341, 385
Podsiadlowski, P., Ivanova, N., Justham, S., & Rappaport, S. 2010, MNRAS, 406, 840
Portegies Zwart, S. F., Verbunt, F., & Ergma, E. 1997, A&A, 321, 207
Remillard, R. A., & McClintock, J. E. 2006, ARA&A, 44, 49
Shao, Y., & Li, X.-D. 2014, ApJ, 796, 37
Shiode, J. H., & Quataert, E. 2014, ApJ, 780, 96

Sion, E. M., Bond, H. E., Lindler, D., et al. 2012, ApJ, 751, 66
Smith, L. F., Biermann, P., & Mezger, P. G. 1978, A&A, 66, 65
Smith, N., & Arnett, W. D. 2014, ApJ, 785, 82
Smith, N., Li, W., Filippenko, A. V., & Chornock, R. 2011, MNRAS, 412, 1522
Sukhbold, T. & Woosley, S. E. 2014, ApJ, 783, 10
Taam, R. E. & Sandquist, E. L. 2000, ARA&A, 38, 113
Tauris, T. M., & Dewi, J. D. M. 2001, A&A, 369, 170
Thorne, K. S. 1974, ApJ, 191, 507
Timmes, F. X., Woosley, S. E., Weaver, T. A. 1996, ApJ, 457, 834
van den Heuvel, E. P. J. 1983, in Accretion-Driven Stellar X-ray Sources, ed. W. H. G. Lewin & E. P. J. van den Heuvel (Cambridge and New York, Cambridge University Press), p. 303
Vink, J. S., de Koter, A., & Lamers, H. J. G. L. M. 2001, A&A, 369, 574
Webbink, R. F. 1984, ApJ, 277, 355
Wijnands, R., in't Zand, J. J. M., Rupen, M., et al. 2006, A&A, 449, 1117
Wiktorowicz, G., Belczynski, K., & Maccarone, T. J. 2013, arXiv:1312.5924v2
Wong, T.-W., Valsecchi, F., Ansari, A., et al. 2014. ApJ, 790, 119
Woosley, S. E., & Weaver, T. A. 1995, ApJS, 101, 181
Xu, X.-J., & Li, X.-D. 2010a, ApJ, 722, 1985
Xu, X.-J., & Li, X.-D. 2010b, ApJ, 716, 114
Yungelson, L. R., & Lasota, J.-P. 2008, A&A, 488, 257
Zhang, S. N., Cui, W., & Chen, W. 1997, ApJ, 482, L155
Zorotovic, M., Schreiber, M. R., Gäsicke, B. T. et al. 2011, A&A, 536, L3

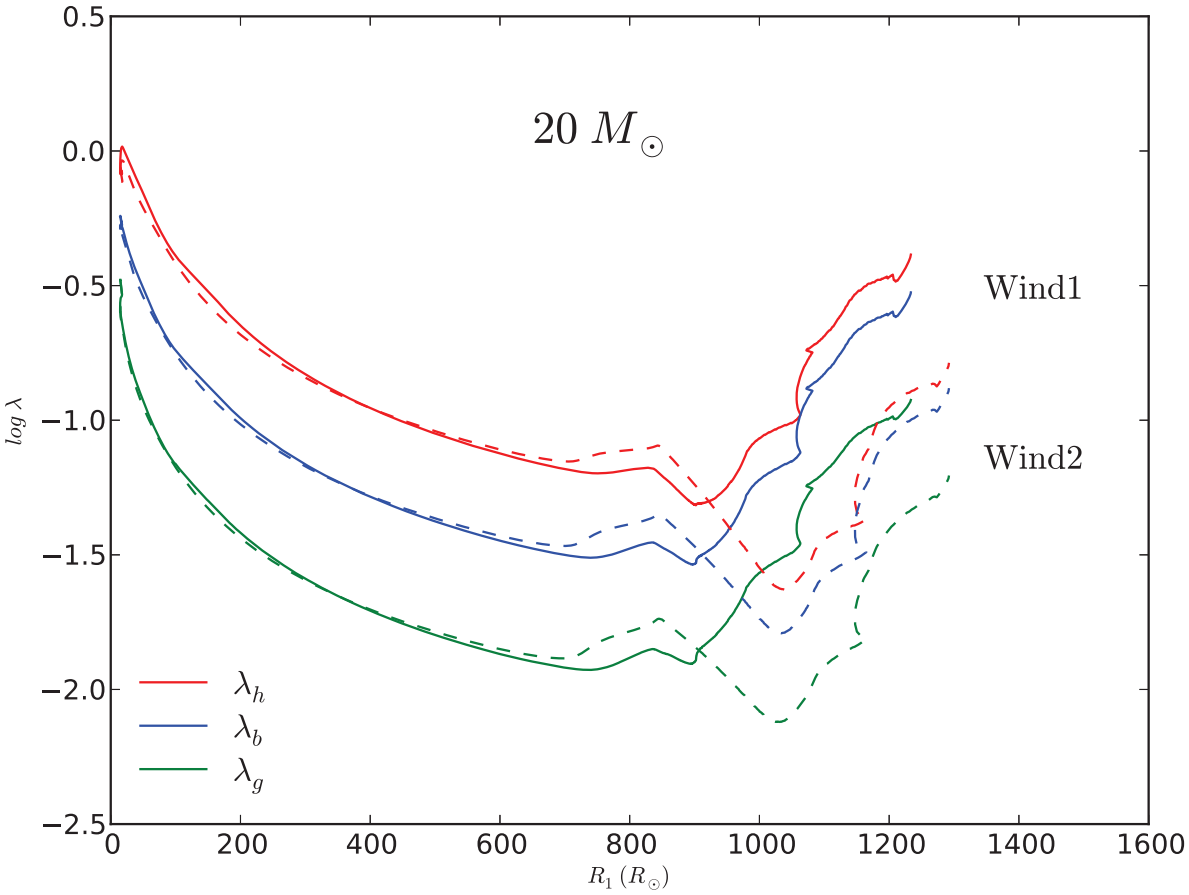

Figure 1. Evolution of the three types of binding energy parameters λ with the stellar radius R for a Pop. I star with initial mass of 20 $M_\odot$. The the red, blue and green lines represent $\lambda_{\rm h}$, $\lambda_{\rm b}$, and $\lambda_{\rm g}$, and the solid and dashed lines represent the results with the Wind1 and Wind2 prescriptions, respectively.

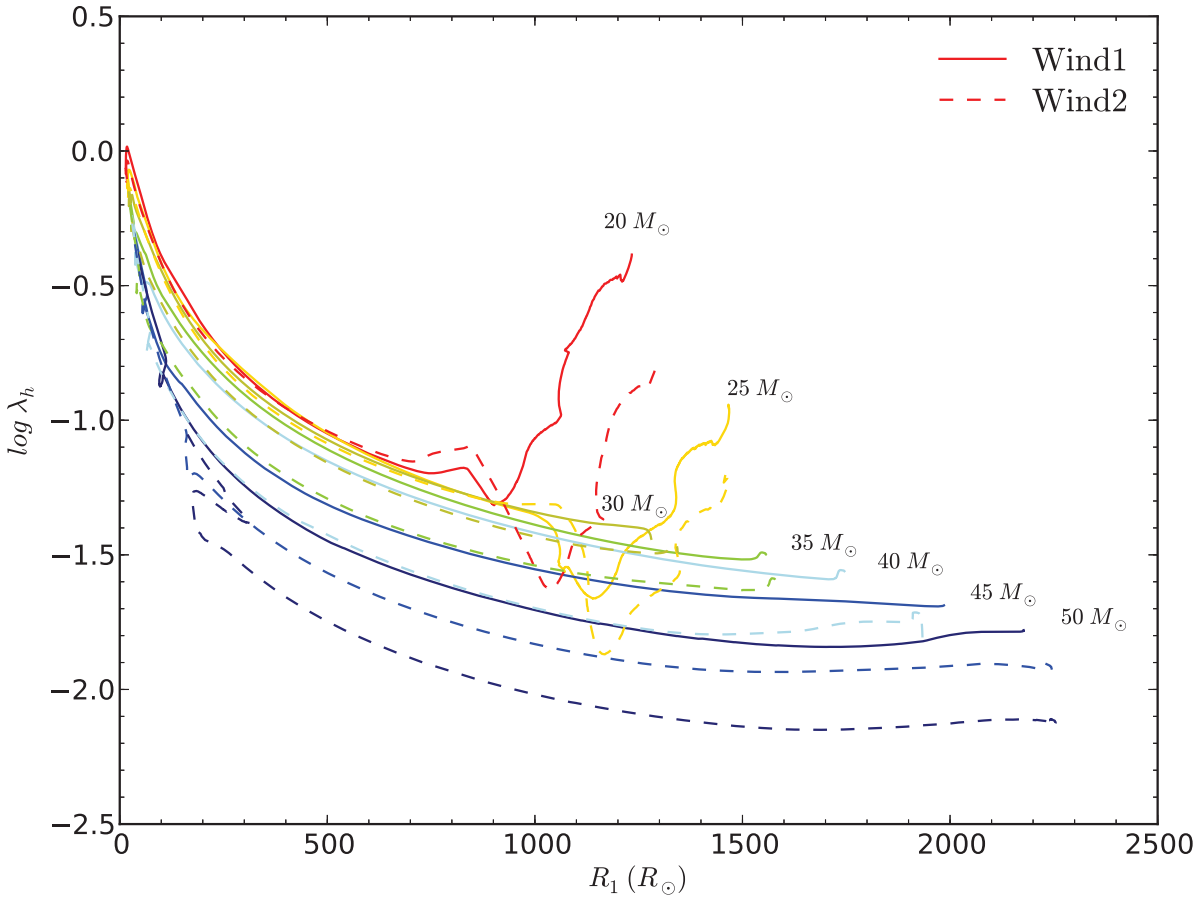

Figure 2. The $\lambda_{\rm h}$ values as a function of the stellar radius for stars with different mass. The solid and dashed lines represent the results with the Wind1 and Wind2 prescriptions, respectively.

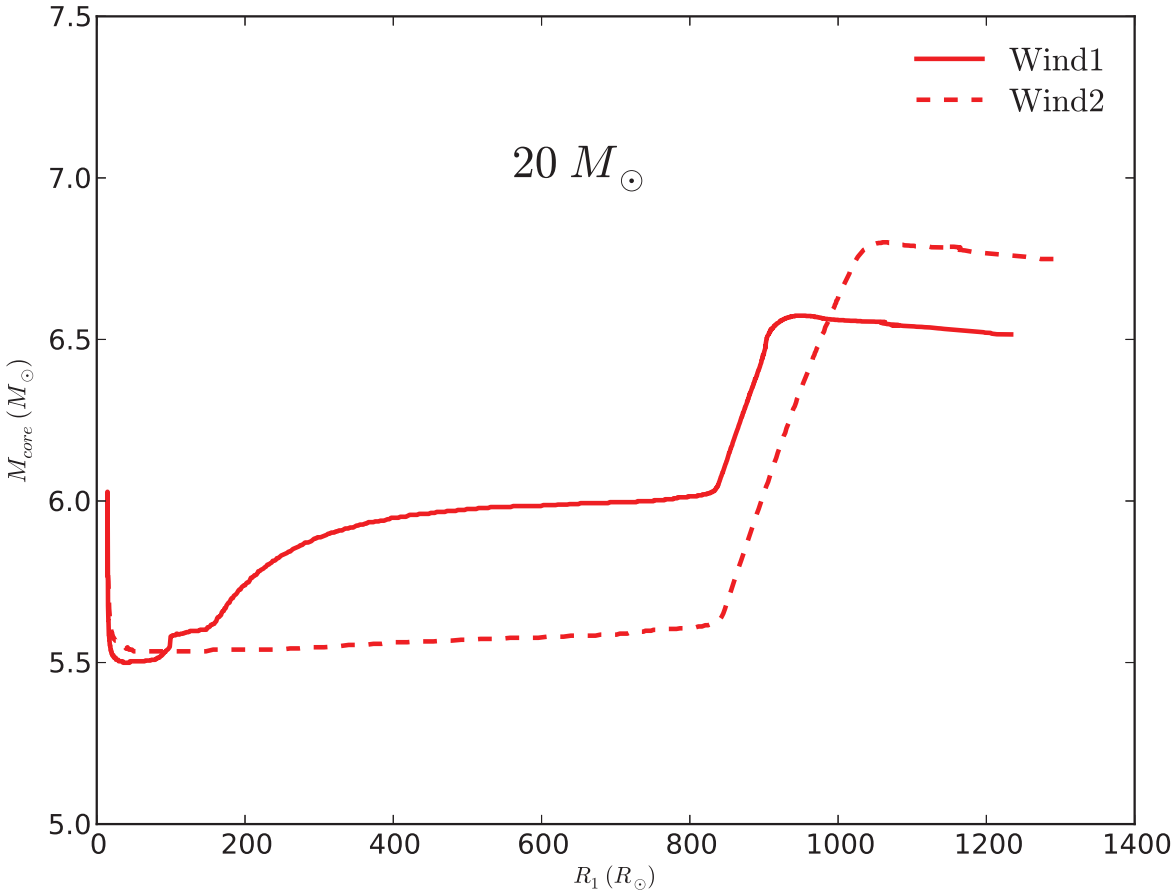

Figure 3. The core mass as a function of the stellar radius for a $20\,M_\odot$ star. Here, the boundary of the core and the envelope is determined to be the maximal compression point in the hydrogen burning shell. The solid and dashed lines represent the results with the Wind1 and Wind2 prescriptions, respectively.

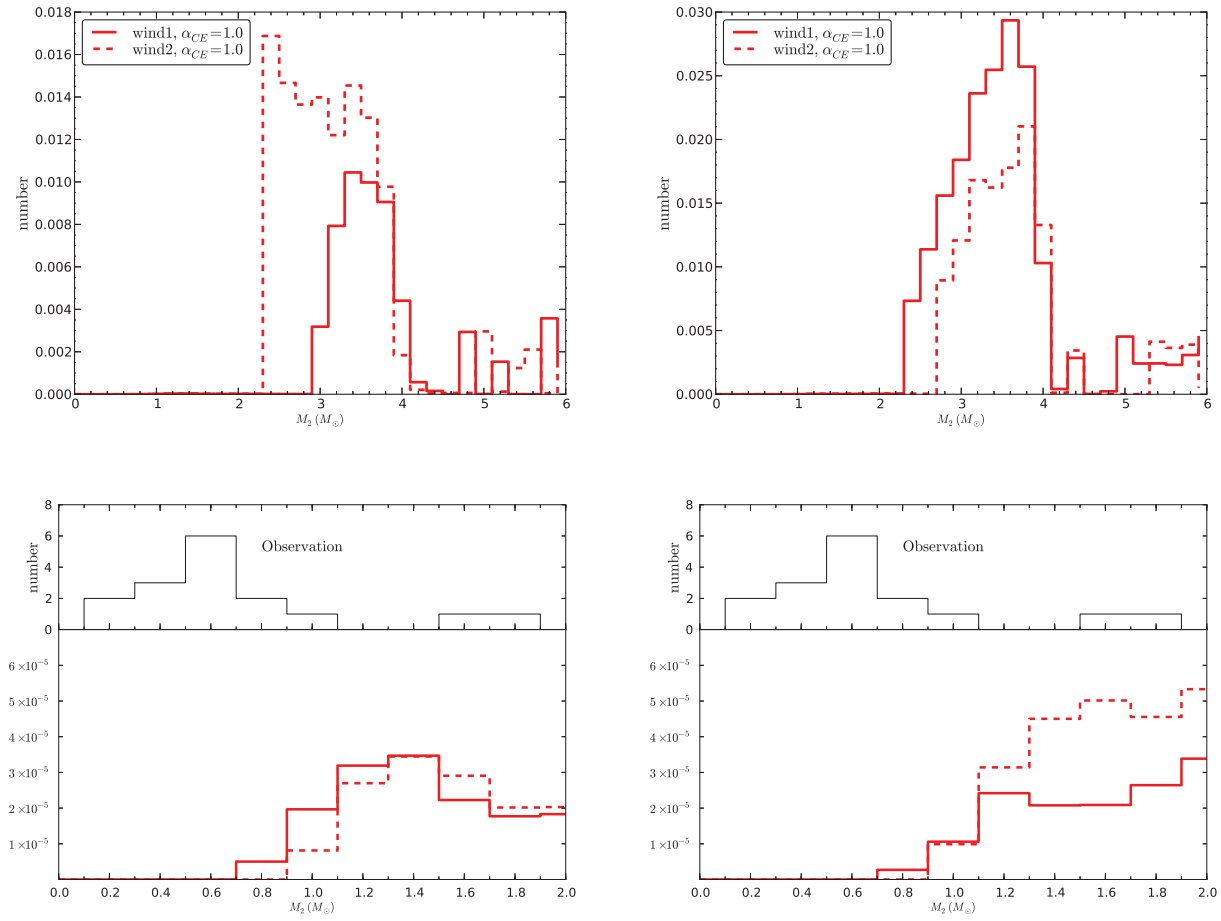

Figure 4. Distributions of the donor mass for the BH XRBs in models A1 (left) and A2 (right). The solid and dashed red lines stand for the results with the Wind1 and Wind2 prescriptions, respectively. Also shown is the donor mass distribution of observed LMXBs in the black line.

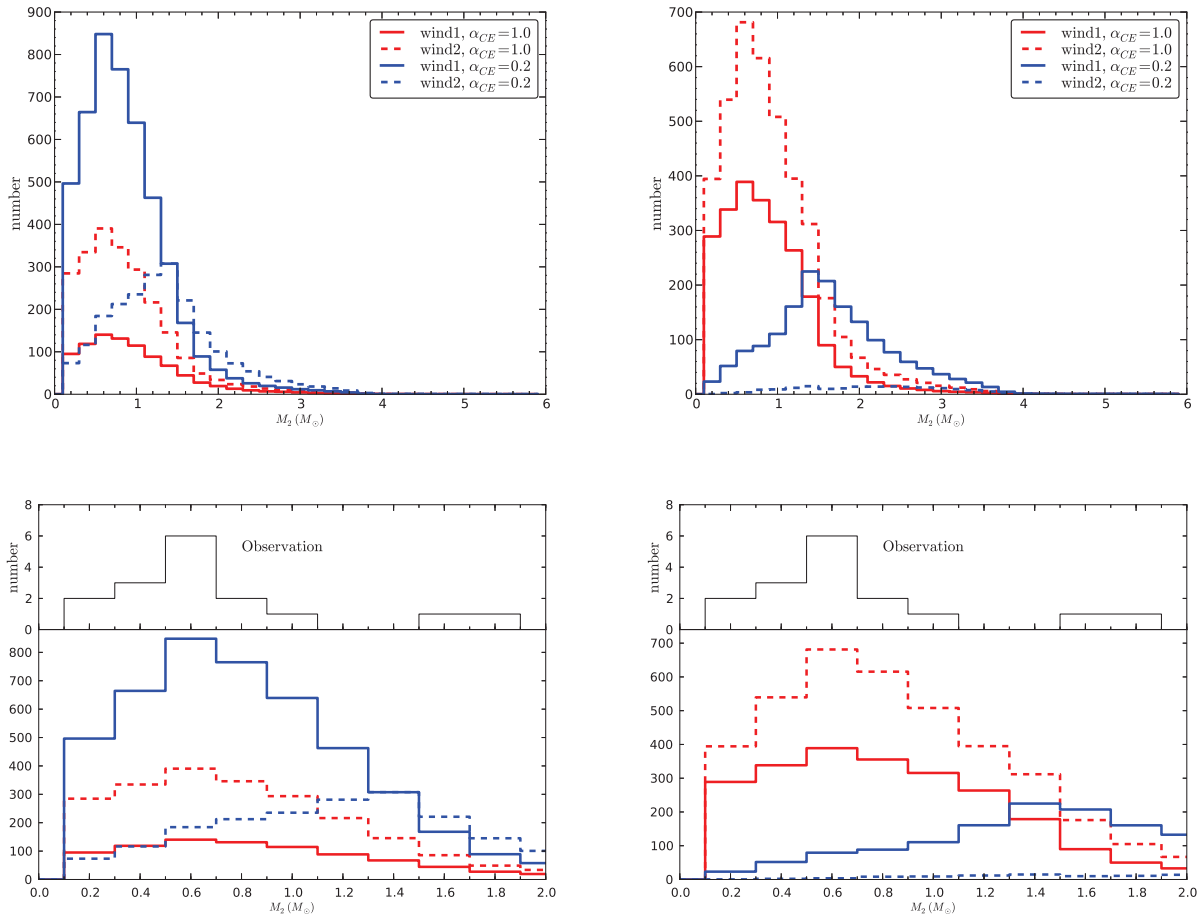

Figure 5. Same as Fig. 3, but for models B1 (left) and B2 (right).

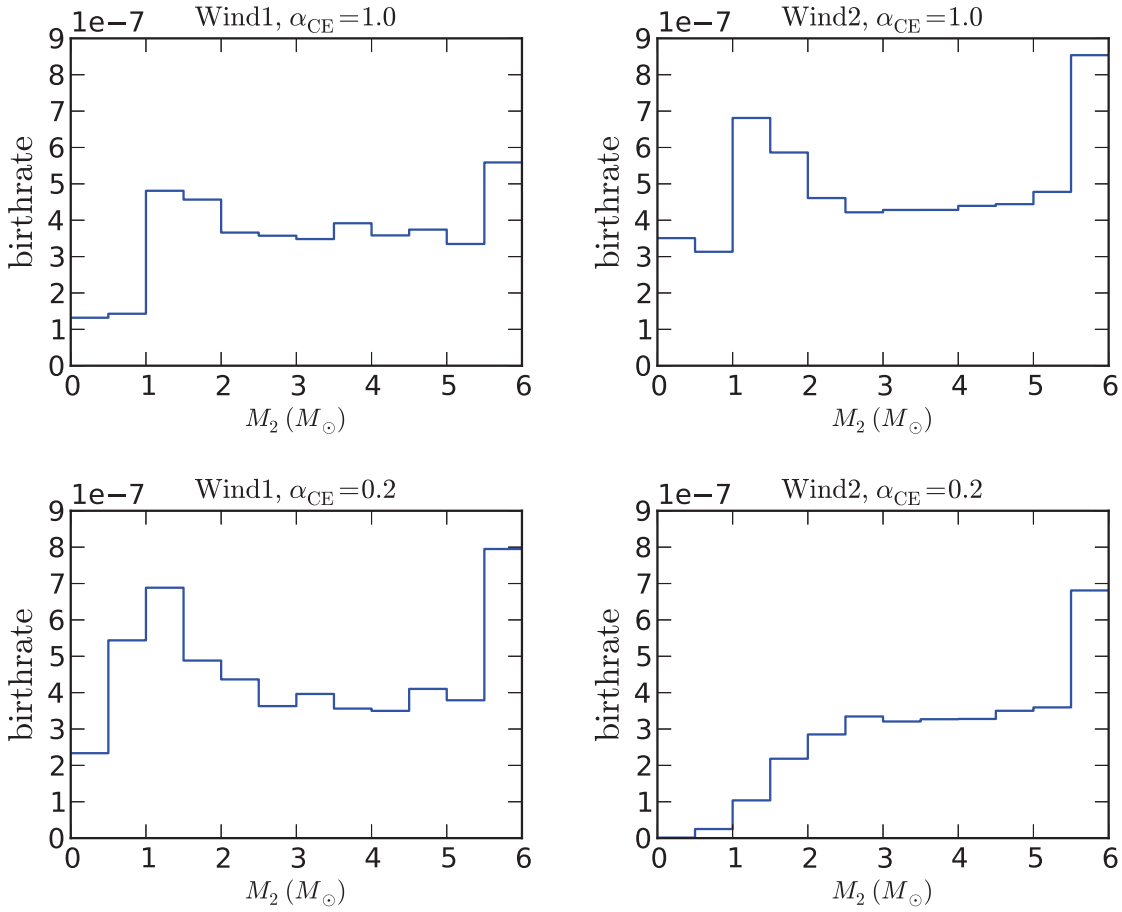

Figure 6. The birthrate of the BH XRBs as a function of the donor masses for model B1 with different wind loss prescriptions and CE efficiencies.

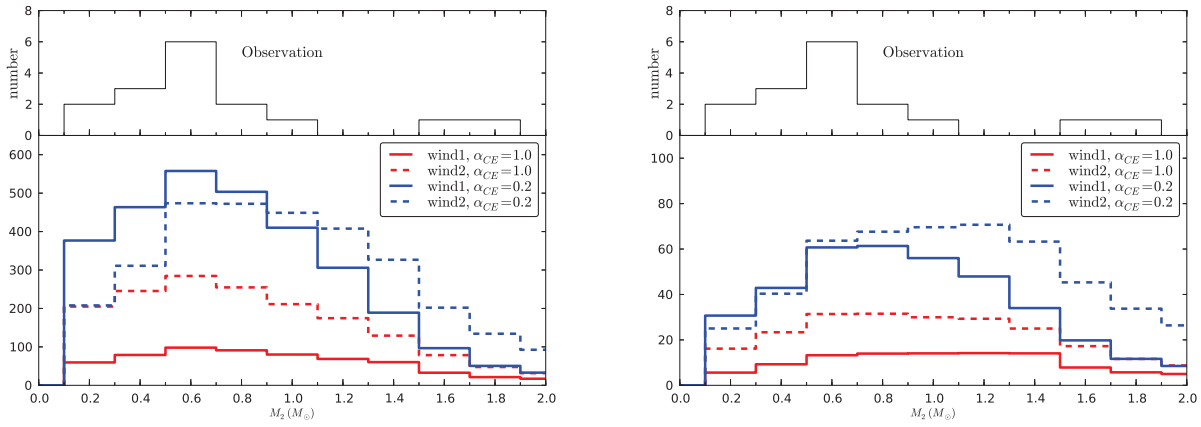

Figure 7. Same as Fig. 3, but for models C1 (left) and C2 (right).

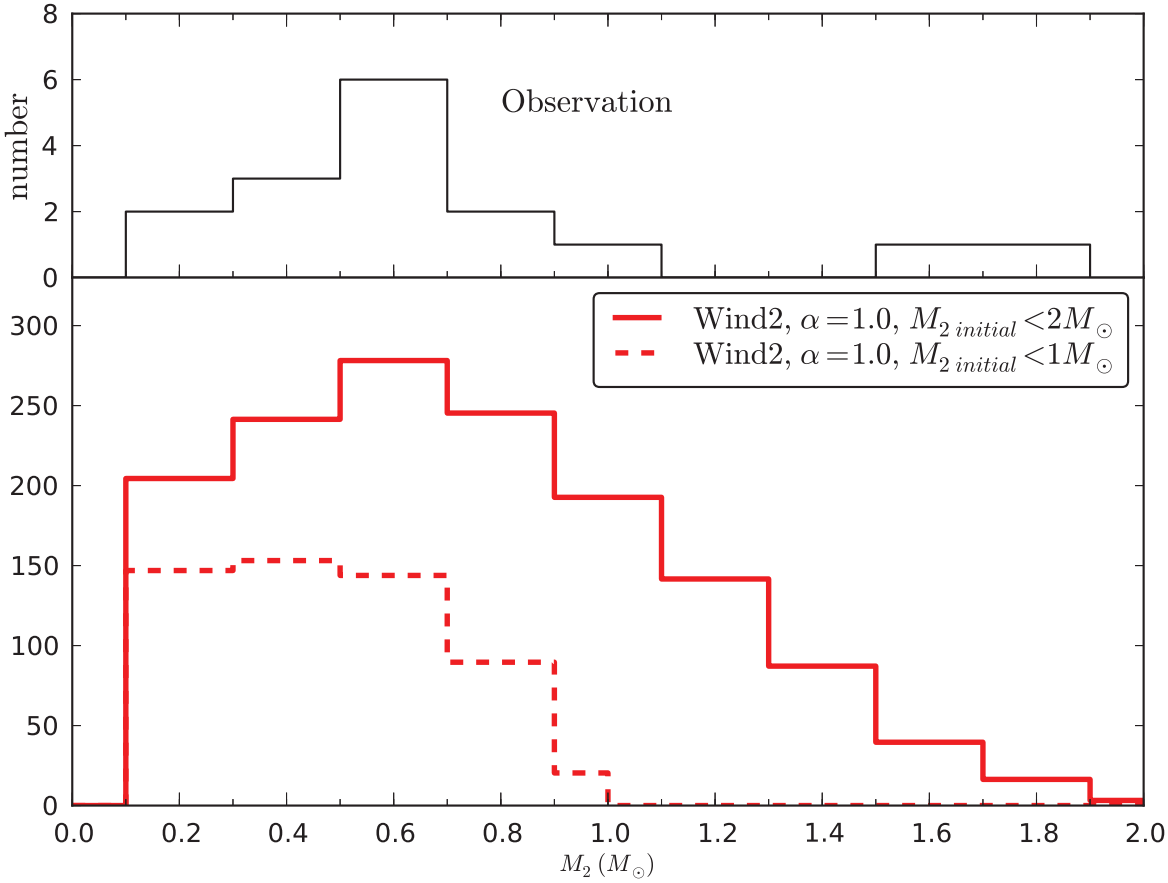

Figure 8. Distributions of the donor masses for BH XRBs in model C1. The solid and dashed lines represent the binaries with initial donor mass $< 2\,M_\odot$ and $< 1\,M_\odot$, respectively.

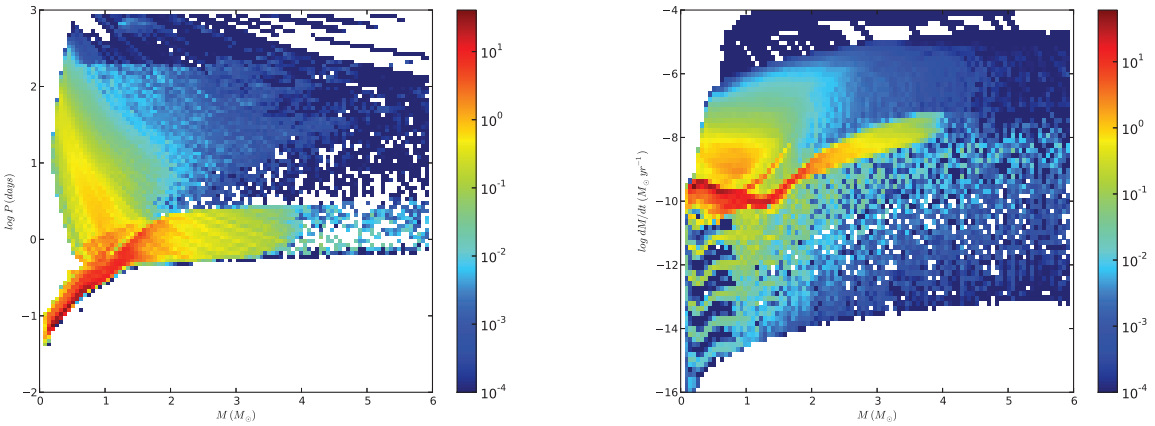

Figure 9. Distributions of the orbital period vs. the donor mass (left panel) and the mass transfer rate vs. the donor mass (right panel) in model C1. The color scale indicates the relative number of XRBs.

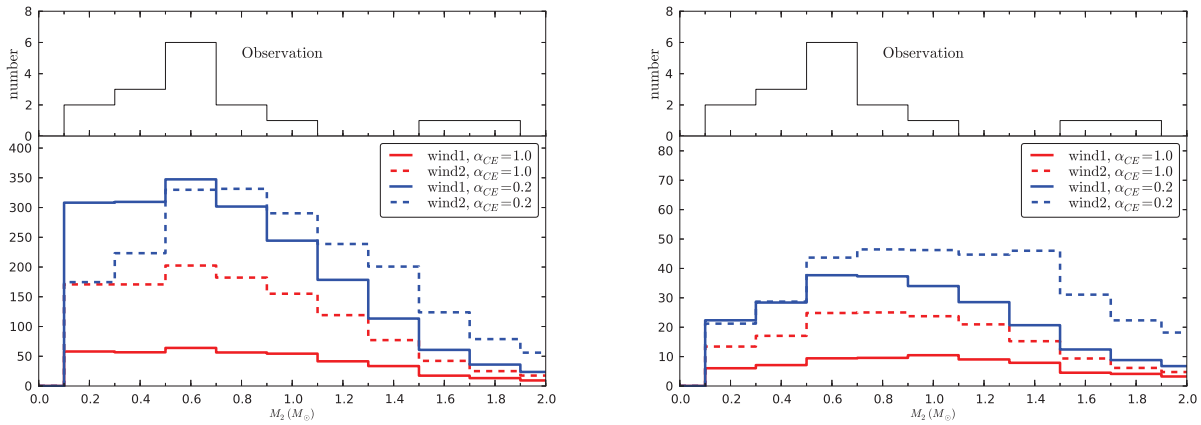

Figure 10. Same as Fig. 3, but for models D1 (left) and D2 (right).

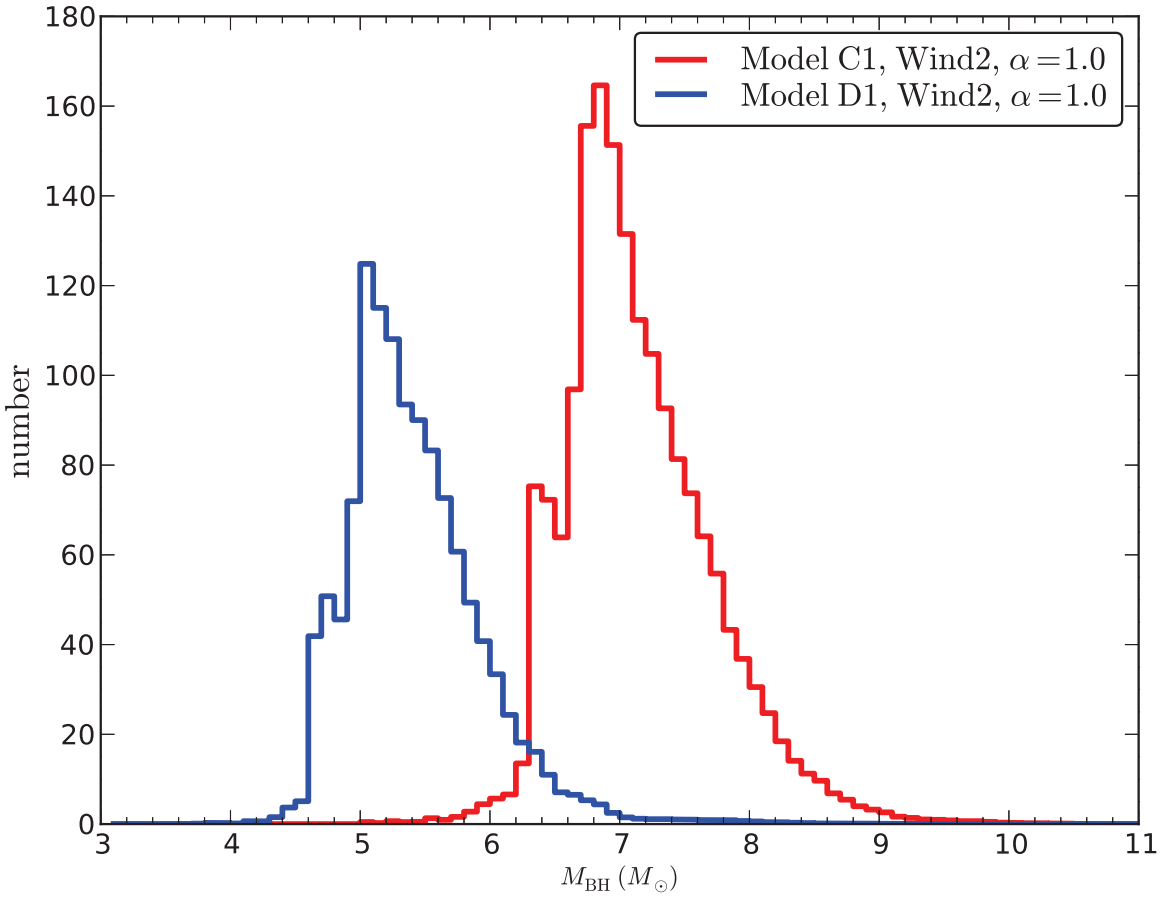

Figure 11. Distributions of the BH mass in models C1(red) and D1 (blue).

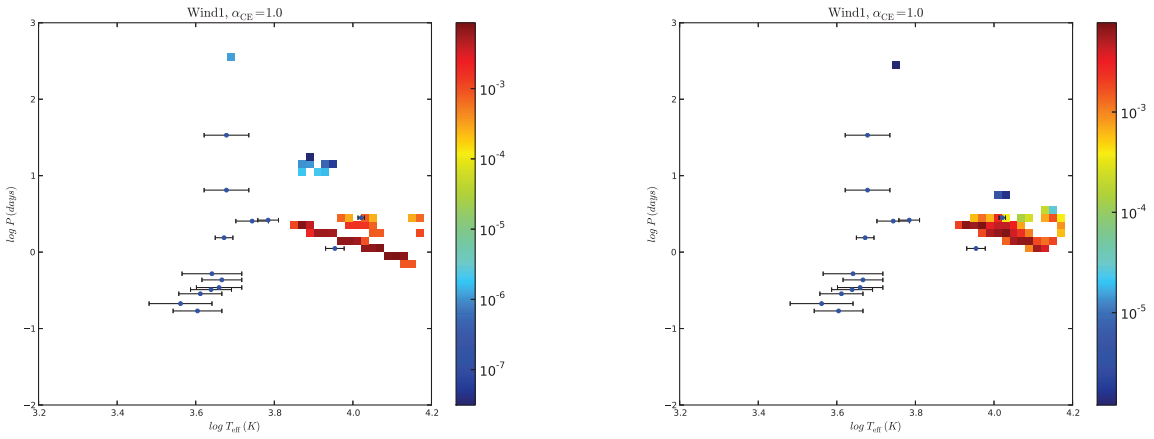

Figure 12. Distribution of the orbital period and the donor star's effective temperature for models A1 (left panel) and A2 (right panel) with the Wind1 prescription and $\alpha_{\rm CE}=1$. The color scale reflects the relative number of the binaries. For comparison, we also plot the measured orbital periods and effective temperatures of Galactic BH LMXBs.

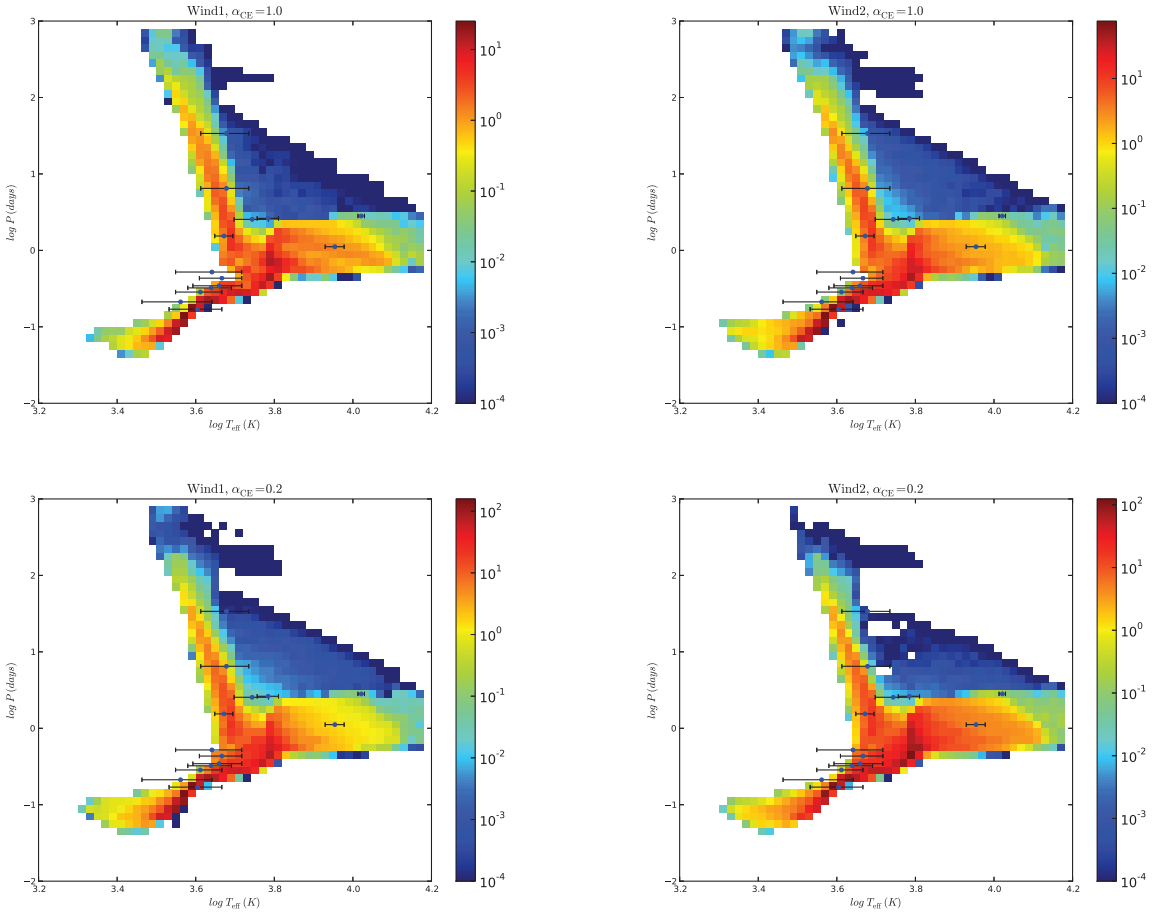

Figure 13. Comparison between the measured and calculated orbital periods and donor star's effective temperatures in model C1 with different input parameters..

Table 1. The stellar parameters for a 20 $M_\odot$ star at different evolutionary stages. Columns 2-4 and 5-7 correspond to the Wind1 (left) and Wind2 (right) prescriptions, respectively

$R\,(R_\odot)$	$M\,(M_\odot)$	$M_{\rm core}\,(M_\odot)$	$\lambda_{\rm h}$	$M\,(M_\odot)$	$M_{\rm core}\,(M_\odot)$	$\lambda_{\rm h}$
52	19.414	5.504	0.675	18.830	5.535	0.602
600	18.738	5.984	0.075	18.787	5.580	0.077
1066	14.098	6.548	0.152	11.72	6.801	0.027
1230	14.096	6.516	0.389	11.54	6.760	0.126

Table 2. Input and derived parameters in the adopted models

Models	$M_{\rm rem}$	λ	$n(q)$	birthrate ($\rm yr^{-1}$)	$D_{\rm cr}(0.001)$	$D_{\rm cr}(0.05)$	D
A1	Eq. (8)	$\lambda_{\rm b}$	1	2.80×10^{-8}			
A2	Eq. (8)	$\lambda_{\rm h}$	1	3.57×10^{-8}			
B1	$M_{\rm He}$	$\lambda_{\rm b}$	1	5.89×10^{-6}	0.488	0.341	0.232
B2	$M_{\rm He}$	$\lambda_{\rm g}$	1	6.54×10^{-6}	0.488	0.341	0.266
C1	$M_{\rm He}$	$\lambda_{\rm h}$	1	5.51×10^{-6}	0.490	0.342	0.255
C2	$M_{\rm He}$	$\lambda_{\rm h}$	$\propto q$	1.74×10^{-6}	0.502	0.350	0.389
D1	$M_{\rm CO}$	$\lambda_{\rm h}$	1	3.14×10^{-6}	0.491	0.342	0.228
D2	$M_{\rm CO}$	$\lambda_{\rm h}$	$\propto q$	9.68×10^{-7}	0.510	0.355	0.351

Table 3. The Kolmogorov-Smirnov statistic for the orbital period (upper) and effective temperature (lower) in each model. See Table 2 for the values of $D_{\rm cr}(\alpha)$.

Model	Wind1/$\alpha_{\rm CE}=1$	Wind2/$\alpha_{\rm CE}=1$	Wind1/$\alpha_{\rm CE}=0.2$	Wind1/$\alpha_{\rm CE}=0.2$
B1	0.274	0.316	0.355	0.304
B1	0.086	0.108	0.110	0.372
B2	0.315	0.322	0.303	0.405
B2	0.107	0.095	0.519	0.633
C1	0.263	0.290	0.342	0.315
C1	0.129	0.090	0.113	0.215
D1	0.290	0.324	0.335	0.311
D1	0.122	0.119	0.146	0.166

This paper has been typeset from a TEX/LATEX file prepared by the author.